Available online at www.sciencedirect.com
ScienceDirect
Journal of the European Ceramic Society 31 (2011) 913–919
www.elsevier.com/locate/jeurceramsoc

Pressureless synthesis of fully dense and crack-free SiOC bulk ceramics via photo-crosslinking and pyrolysis of a polysiloxane

Sandra Martínez-Crespiera [a], Emanuel Ionescu [a,*], Hans-Joachim Kleebe [b], Ralf Riedel [a]

[a] Technische Universität Darmstadt, Institut für Materialwissenschaft, Petersenstrasse 23, D-64287 Darmstadt, Germany
[b] Technische Universität Darmstadt, Institut für Angewandte Geowissenschaften, Schnittspahnstrasse 9, D-64287 Darmstadt, Germany

Received 10 September 2010; received in revised form 30 October 2010; accepted 21 November 2010
Available online 14 December 2010

Abstract

This paper presents the pressureless preparation of fully dense and crack-free SiOC ceramics via direct photo-crosslinking and pyrolysis of a polysiloxane. Elemental analysis revealed the presence of high levels of carbon in the SiOC ceramics. Thus, the samples showed the highest content (78–86 mol%) of segregated "free" carbon reported so far. XRD investigations indicated that the materials prepared at 1100 °C were X-ray amorphous, whereas the sample prepared at 1400 °C contained a turbostratic graphite-like phase and silicon carbide as crystalline phases, as additionally confirmed by TEM and Raman spectroscopy. Vickers hardness was measured to be 5.5–8.6 GPa. The dc resistivity of the prepared material at 1100 °C was 0.35 Ω m, whereas the ceramic pyrolyzed at 1400 °C showed a value of 0.14 Ω m; both values are much lower than those of other known SiOC materials. This latter feature was attributed to the presence of a percolating carbon network in the ceramic.

Keywords: Carbon; Electrical conductivity; Glass ceramics; Polymer derived ceramics (PDCs)

1. Introduction

Polymer derived ceramics (PDCs) are materials which have been intensively studied in the last four decades.[1] They can be prepared by thermal handling of appropriate precursors (preceramic polymers[2]) in inert or reactive atmosphere without using any additives as in the case of conventional ceramics fabricated mainly by sintering techniques.

The overall process for fabrication of PDCs involves four major steps: (i) synthesis of preceramic polymers starting from suitable monomers; (ii) polymer crosslinking at moderated temperatures (100–400 °C) to furnish infusible organic/inorganic hybrid materials (preceramic networks); (iii) shaping and (iv) ceramization process (pyrolysis) of the crosslinked and shaped green bodies, which are converted into inorganic materials by heat treatment at temperatures ranging from 1100 to 1500 °C.[3] During the polymer-to-ceramic conversion a high mass loss is typically observed, which leads to high porosity and high shrinkage in the green bodies. Since preceramic polymers usually have densities of ca. 1 g/cm^3, while the corresponding ceramic materials exhibit densities in the range of 2–3 g/cm^3, the conversion into a ceramic is obviously accompanied by the generation of residual stresses leading to defects and cracking of the ceramic parts.[4] Thus, it is very difficult to produce dense and crack-free monoliths using the polymer derived route. To avoid these problems, the use of passive or active filler particles was proposed in order to act against shrinkage and mass loss and thus allow the production of crack-free monoliths with low residual porosities.[5,6] By combining passive and active fillers, near net shape production of PDC-based parts is possible since zero shrinkage can be achieved.[7] Hence, filler-free PDC-based parts can only be produced either by having high porosity[8] or by keeping the parts very thin.[9]

The fabrication of dense and crack-free PDC-based monoliths has been reported to be possible by using pressure-assisted techniques, such as pressure-assisted casting,[10,11] hot isostatically pressing techniques (HIP)[12] or field assisted sintering technology (FAST).[13] However, by means of these techniques only small parts with simple geometries can be fabricated.

There have been several publications on the pressureless fabrication of dense polymer derived ceramics in the SiOC[9] or SiCN system.[14–16] Here we report for the first time on the

* Corresponding author. Tel.: +49 0 6151 166344; fax: +49 0 6151 166346.
E-mail address: ionescu@materials.tu-darmstadt.de (E. Ionescu).

0955-2219/$ – see front matter © 2010 Elsevier Ltd. All rights reserved.
doi:10.1016/j.jeurceramsoc.2010.11.019

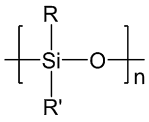

R, R' = -H, aryl, alkyl, vinyl

Fig. 1. Structure of the commercially available polysiloxane Polyramics® RD-684 (Starfire Systems Inc.) as provided by the producer.

filler-free and pressureless production of dense and crack-free SiOC-based monoliths with a thickness up to 1.5 mm via direct photo-crosslinking and subsequent pyrolysis of a commercially available polysiloxane. Since the geometry is determined by the mold used for the liquid polymer, fully dense ceramic parts with complex geometries can be prepared using this rather simple technique.

2. Experimental procedure

Commercially available polysiloxane RD-684 Polyramic® (Starfire Systems Inc.) was used as a preceramic polymer (Fig. 1). The preceramic polymer was first mixed with 5 wt% of the photoinitiator Irgacure® 651 (Ciba) by means of ultrasonic treatment. Subsequently, vacuum was applied to eliminate the generated bubbles. In order to obtain the monolithic specimens, different PTFE crucibles with thicknesses of 2, 2.5 and 4 mm were used. They were filled with the liquid precursor and covered with a transparent glass substrate. The samples were irradiated with a UV Lamp (UVACUBE 200®, Honle, mercury lamp with $I = 30\,mW/cm^2$ and $\lambda = 365\,nm$) for 30 min After demolding, transparent infusible dense crack-free monoliths (3 cm × 3 cm) with thicknesses of 1.5, 2 and 3.5 mm were obtained. The green bodies were pyrolyzed under argon at 1100 °C at a heating rate of 50 °C/h. The samples were placed in the furnace between two graphite felts in order to avoid warping and cracking. Thus, the graphite felts might reduce friction forces due to shrinking of the samples during pyrolysis and simultaneously allow for uniform outgassing of volatiles during ceramization.[11] At the end, dense, flat and crack-free SiOC specimens were obtained with thicknesses up to 1.5 mm.

The chemical analysis of the polymer was performed at the Mikroanalytisches Labor Pascher (Remagen, Germany). Elemental analyses for carbon and oxygen were performed using a LECO C-200 and a LECO TC-436 analyzer, respectively.

The pyrolytic transformation from the polymer to the ceramic was studied by thermo gravimetric analysis (TGA) using Netzsch STA 429C Jupiter® equipment operating in argon flux (25 ml/min) at a heating rate of 5 °C/min up to the max. temperature of 1400 °C. Analysis of the evolved gases was performed *in situ* using a coupled quadrupole mass spectrometer (QMS 403C Aeolos).

The density of the ceramic samples was analyzed geometrically and by means of liquid pycnometry (water) and Hg-pressure porosimetry. The residual porosity in the ceramics was measured by a mercury pressure porosimeter (Micrometrics poresizer 9320) and by the BET (Brunauer-Emmett-Teller) method with a Quantachrome Autosorb 3B surface area analyzer.

Powder X-ray diffraction (XRD) of the ceramic samples was performed with a STOE X-ray diffractometer using Ni-filtered Cu Kα radiation.

Micro-Raman spectra (10 scans, each lasting 3 s) were recorded using a Horiba HR800 micro-Raman spectrometer equipped with an air-cooled Melles Griot argon laser (irradiation wavelength 514.5 nm). The excitation line has its own interference filter (to filter out the plasma emission) and a Raman notch filter (for laser light rejection). The measurements were performed with a grating of 1800 g mm^{-1} and a confocal microscope (magnification 100×, NA 0.5) with a 100 μm aperture, giving a resolution of 2–4 μm. The laser power (ca. 20 mW) on the sample was attenuated using neutral density (ND) filters in the range of 2 mW–20 μW.

Scanning electron microscopy (SEM) measurements were performed with a Philips XL30FEG SEM microscope. The samples were sputtered with a thin gold layer before the SEM investigation. Transmission electron microscopy (TEM) imaging was performed using a Philips CM20STEM (FEI, Eindhoven, The Netherlands) operating at 200 keV on TEM-foils obtained from the pyrolyzed SiOC bulk samples. Sample preparation followed the standard ceramographic technique of cutting, ultrasonic drilling, dimpling and Ar-ion thinning to perforation followed by light carbon coating to minimize charging under the incident electron beam.

Vickers hardness of the bulk SiOC samples was evaluated by the indentation method using a Vickers diamond pyramid indenter (Otto Wolpert Werke) under various loads (0.5–20 N, loading time 15 s.). Nanoindentation experiments were performed with a Picoindentor® HM500 device (Fischer) equipped with a diamond pyramid Berkovich indenter to measure the hardness and the Young's modulus of the ceramic samples. The experiments were carried out with a max. load of 300 mN during 5 s. The elastic modulus was calculated as an average, using the experimentally determined continuous stiffness measurements.

The linear four-point probe technique using a Lucas Signatone QuadPro Resistivity System (Lucas-Signatone Corp.) was applied to obtain the dc resistivity of the SiOC samples at room temperature.

3. Results and discussion

The crosslinking of the polysiloxane RD-684 was performed via UV light irradiation (wavelength 365 nm). Photoinitiator Irgacure 651 was used as a sensitizer (5 wt%), since it generates radicals upon UV exposure. The generated radicals can activate the vinyl groups of the polysiloxane to react and polymerize, yielding a three dimensional infusible network. Furthermore, other crosslinking mechanisms known for polysiloxanes (such as hydrosilylation or dehydro coupling reactions)[3] can also be initiated under these conditions. Whereas vinyl polymerization and hydrosilylation reaction occur without mass loss, the dehydro coupling reactions lead to hydrogen release, which was determined via *in situ* mass spectrometry during thermogravimetric analysis of the polymer (see below). The polymeric

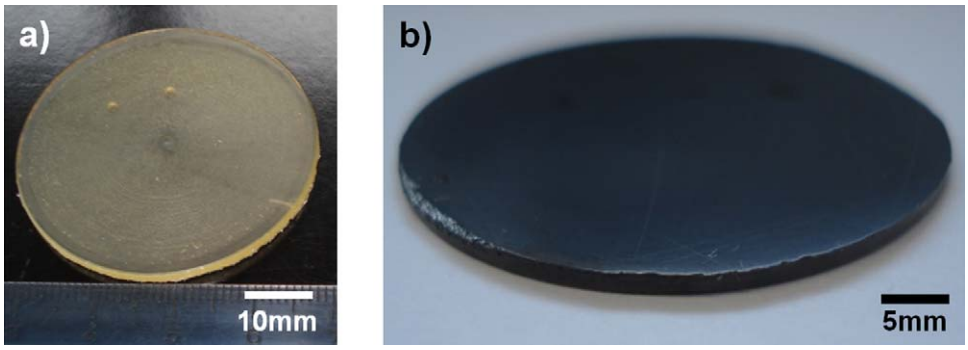

Fig. 2. Optical photographs of (a) the green body after photo-crosslinking of polysiloxane Polyramics RD-684 and (b) of the SiOC ceramic (thickness 1.5 mm, diameter 34 mm) after pyrolysis.

samples were irradiated with UV light for 20 min to obtain transparent infusible monoliths (green-bodies) which were easily removed from the Teflon crucible and the glass substrate. When irradiated for a longer time, the samples were found to crack upon demolding. Subsequently, the free-standing bulk green bodies were irradiated for an additional 10 min on each side to ensure complete crosslinking. They were finally pyrolyzed in argon atmosphere at 1100 °C to furnish dense crack-free silicon oxycarbide specimens (Fig. 2).

Fig. 3 shows the TG curve of the UV cured infusible polymer RD-684 (with 5 wt% Irgacure added) from ambient temperature to 1400 °C. The polymer-to-ceramic transformation induces a total weight loss of 40 wt%, which occurs in two main decomposition steps in the temperature region between 350 °C and 750 °C, as shown by the DTG curve (Fig. 3). The high mass loss is due to the release of hydrocarbons (vinyl—$m/z = 26$, 27; phenyl—$m/z = 50$, 51, 52, 77, 78; methyl—$m/z = 14$, 16; propyl—$m/z = 37$) and hydrogen, as indicated by *in situ* mass spectrometry investigation.

Although different PTFE molds with thicknesses up to 3.5 mm were tested, only the monoliths with thicknesses up to 1.5 mm did not crack during pyrolysis. This behavior can be explained by considering the amount of evolved gases during pyrolysis. If the surface-to-volume ratio of the green body is too

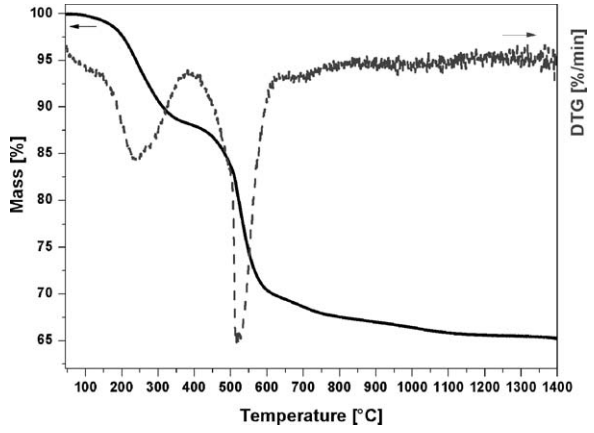

Fig. 3. TG and DTG (first time derivative of TG) curves of the UV-cured preceramic polymer (RD-684 + 5 wt % Irgacure 651) from room temperature up to 1400 °C.

low, the removal of the gaseous by-products can be hindered with the result of interior pressure increase and crack formation. Furthermore, it should be noted that despite of relatively high mass loss of the polymer during ceramization, the residual porosity of the ceramic parts is negligible.

The largest crack-free SiOC ceramic part we have obtained showed a diameter of 3.4 cm and a thickness of 1.5 mm. The linear shrinkage of the green body upon pyrolysis was found to be 20% and the weight loss of the part (35 wt%) was ca. 12% lower than that determined by TGA measurements. This can be explained by the additional UV irradiation of the green bodies after demolding, a process which increases the crosslinking grade in the green parts and thus leads to an increase in their ceramic yield. The effect of the different heating rate used (i.e. 5 °C/min for TGA and 0.8 °C/min upon pyrolysis) can probably be excluded since the ceramic parts were annealed for 1 h upon pyrolysis, whereas during TGA cooling was started immediately after reaching the maximal temperature. Thus, the pyrolysis process is expected to lead to a higher mass loss than that recorded by TGA. This has been shown also in other cases, as for polymer derived SiOC/ZrO_2 and SiOC/HfO_2 nanocomposites. Whereas the mass loss of the ceramic pyrolyzed at 1100 °C upon annealing at 1600 °C was 10.8 and 8.5 wt%, respectively (heating rate 1 °C/min),[17,18] mass losses of only 1 wt% and 0.38 wt%, respectively were recorded at 2000 °C via high temperature TGA (heating rate 5 °C/min).[19] Since the opposite trend was observed in our case, the increased crosslinking grade in the green parts (which was induced by the intensive UV irradiation of the green bodies) is most probably the reason for the low mass loss upon ceramization.

The chemical compositions and empirical formulae of the polymer as well as those of the ceramic materials obtained upon pyrolysis at 1000 °C, 1100 °C and 1400 °C are summarized in Table 1. The hydrogen content in the sample pyrolyzed at 1000 °C was found to be relatively high (0.53 wt%). However, by increasing the pyrolysis temperature to 1100 °C, the hydrogen content in the ceramic decreases notably. Interestingly, the addition of the photoinitiator to the polysiloxane leads to a remarkable decrease in the hydrogen content compared to that of a ceramic sample prepared without the addition of Irgacure. Furthermore, the addition of Irgacure® to the polysiloxane induces the increase of the carbon content in the SiOC sample from

Table 1
Elemental analysis of the polymer RD-684 and of the SiOC ceramics prepared upon pyrolysis at different temperatures.

Sample	Content in wt%				Empirical formula*	Calculated content in mol%		
	Si	O	C	H		SiO_2	SiC	C_{free}
RD-684	22.65	13.10	57.45	6.00	$SiOC_{5.84}H_{7.32}$	–	–	–
1000 °C	28.35	20.00	49.75	0.53	$SiO_{1.24}C_{4.10}H_{0.52}$	13.14	8.05	78.81
1100 °C	22.10	16.71	61.19	0.09	$SiO_{1.32}C_{6.43}H_{0.11}$	9.31	4.80	85.89
1100 °C (no addition of Irgacure®)	29.01	16.90	51.56	0.28	$SiO_{1.02}C_{4.15}H_{0.27}$	11.89	9.34	78.77
1400 °C	25.32	17.52	57.16	–	$SiO_{1.06}C_{4.60}$	10.37	6.63	83.00

* Normalized to one silicon atom.

51.56 wt% in the ceramic without the initiator to 61.19 wt% in the material pyrolyzed in the presence of Irgacure®.

Considering oxygen bonded to silicon and the rest of silicon bonded to carbon, the amount of "free" carbon can be estimated (Table 1). Thus, for a chemical composition $Si_xO_yC_z$, the molar fractions of SiC, SiO_2, and "free" carbon were calculated, as presented in Table 2.[20] The prepared ceramics show a remarkably high content of carbon, thus a significant amount of free carbon is present. Carbon-rich polymer derived ceramics have been claimed to exhibit interesting and intriguing behavior with respect to their microstructure,[21] thermo-mechanical properties[22] or crystallization resistance[23] at high temperatures. To the best of our knowledge, the presented ceramics show the highest carbon content measured as yet in SiOC-based materials. Whereas in the case of our samples carbon mol fractions of 78 to ca. 86% were observed, other carbon-rich SiOC materials reported in the literature show carbon contents up to max. 73 mol%.[24,25]

The porosity of the SiOC ceramic pyrolyzed at 1100 °C was studied by BET, mercury intrusion porosimetry and SEM. The BET analysis revealed a surface area less than 1 m^2/g, indicating that the bulk SiOC ceramic does not contain any micropores, mesopores or open porosity. Furthermore, the BET analysis shows a Type VI isotherm, which is typical for layer-by-layer adsorption on a uniform surface of a non-porous material (Fig. 4).

In agreement with the porosity analysis, SEM investigation indicated that the SiOC ceramic is fully dense and exhibits a quite smooth surface (Fig. 5).

The density of the prepared ceramic parts was evaluated via pycnometry, Hg-pressure porosimetry and geometrically. All three methods indicate a density of 1.6–1.7 g/cm^3. This value is quite low compared to other SiOC ceramics (2.1 to 2.3 g/cm^3).[19,21,26–28] The low density of our SiOC ceramic can

Table 2
Calculated mol fractions of SiO_2, SiC and free carbon in SiOC ceramics using their chemical composition.

$Si_xO_yC_z$	Amount (mol)	Mol fraction (%)
SiO_2	$y/2$	$y/(2z+y) \times 100$
SiC	$x-(y/2)$	$2[x-(y/2)]/(2z+y) \times 100$
"free" C	$z-[x-(y/2)]$	$2\{z-[x-(y/2)]\}/(2z+y) \times 100$
Total	$z+(y/2)$	100

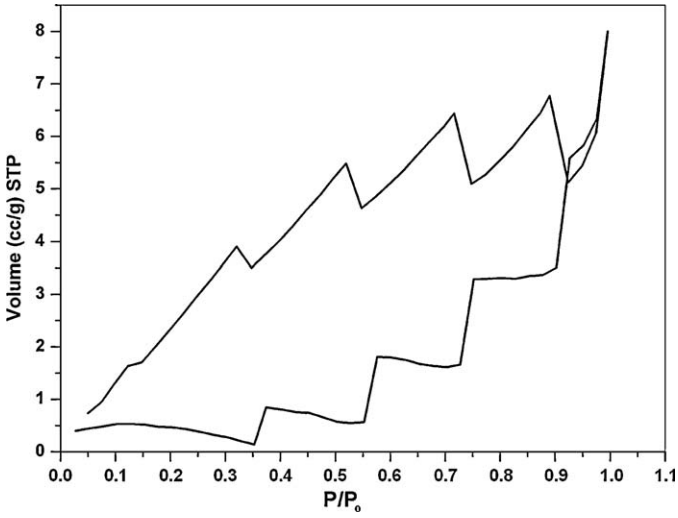

Fig. 4. N_2 adsorption isotherm of the SiOC ceramic pyrolyzed at 1100 °C obtained by the BET method.

be attributed to the unusually high carbon content. Based on the elemental analysis data, a density value of ca. 1.8 g/cm^3 can be calculated in the case of the SiOC sample pyrolyzed at 1100 °C and consisting of 31 wt% of amorphous SiO_2 (density ca. 2.2 g/cm^3),[29] 11 wt% of amorphous SiC (ca. 3.1 g/cm^3)[30] and 58 wt% of segregated carbon (1.45 g/cm^3 for amorphous, pyrolytic carbon).[31] This result matches quite well with the experimental values Fig. 6.

The SiOC ceramic samples prepared upon pyrolysis at 1100 and 1400 °C were investigated with respect to their microstructure by means of transmission electron microscopy (TEM). The sample pyrolyzed at 1100 °C presented a completely amorphous microstructure (not shown here), as reported usually for polymer derived ceramics prepared upon pyrolysis at 1000–1100 °C showing random glass network.[32,33] However, the ceramic pyrolyzed at 1400 °C showed the presence of β-SiC crystallites with a size of 1–4 nm, whose presence was confirmed by electron diffraction analysis. Furthermore, a percolation network of turbostratic carbon was also identified within the sample microstructure (with an interplanar distance of approximately 0.33 nm between the graphene layers perpendicular to the *c*-axis). It should be noted that different defocus settings were utilized in order to image either β-SiC or turbostratic carbon. Whereas for imaging of carbon the defocus was ca. −5 nm (Gauss defocus), a defocus value of ca. −40 nm (close to

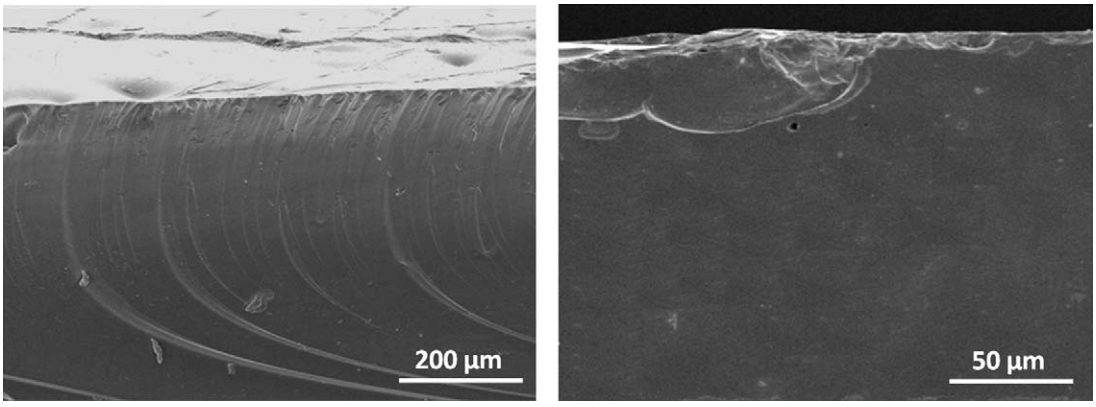

Fig. 5. SEM micrographs of the SiOC ceramic pyrolyzed at 1100 °C.

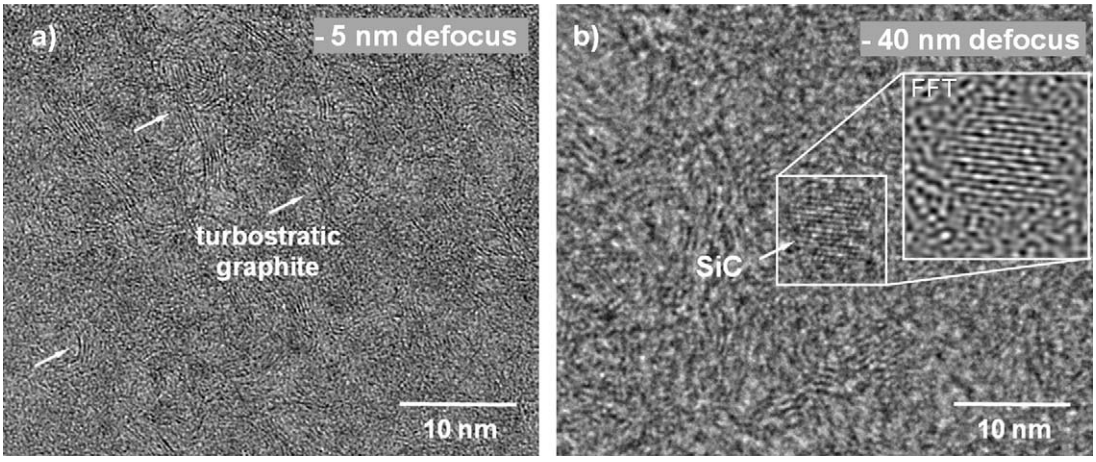

Fig. 6. TEM micrographs of the SiOC ceramic pyrolyzed at 1400 °C showing the turbostratic carbon (left-defocus −5 nm) and the β-SiC phase (right-defocus −40 nm). Note that both images reveal the very same sample area.

Scherzer defocus) was used to image the silicon carbide phase. The overall microstructure of the SiOC sample produced upon pyrolysis at 1400 °C is similar to that of other carbon-rich SiOC materials.[18,21,29]

The SiOC ceramic samples pyrolyzed at 1100 and 1400 °C were investigated with respect to their crystalline phase composition by means of powder XRD (Fig. 7). The samples prepared upon pyrolysis at 1100 °C were found to be X-ray amorphous. The SiOC produced at 1400 °C revealed the presence of β-SiC-nanocrystallites with diffraction reflexes at $2\Theta = 35.6°$ (1 1 1), 60.1° (2 2 0), 71.9° (3 1 1) and 75.7° (2 2 2) and having a size of 1–2 nm (as calculated by Debye-Scherer equation). Furthermore, a turbostratic graphitic-like phase[34] was found to be present in the sample, with a main diffraction reflex at $2\Theta \approx 43°$. Thus, the XRD data support the TEM results.

The presence of the carbon phase in the SiOC sample prepared at 1400 °C was also clearly supported by Raman spectroscopy (Fig. 8). The Raman spectrum of the SiOC materials showed the presence of two high intensity bands at ca. 1350 and 1590 cm^{-1}, corresponding to typical vibration modes in carbon-based materials, i.e. disorder-induced (D) and graphitic-like (G) mode, respectively.[35–37] The ratio of the intensities of the D and G bands was determined to be 2.5. Applying the equation proposed by Ferrari and Robertson,[30] the carbon cluster size (L_a—size of carbon domains along the six fold ring plane, i.e. lateral size), was determined to be 2.1 nm. This value is comparable with cluster sizes observed in other carbon-rich polymer derived ceramics.[20] It is interesting to note that this value of the carbon cluster size is slightly underestimated; the actual lateral size was imaged by TEM approximately by a factor of 2–3× larger.

The Vickers hardness of the SiOC ceramic pyrolyzed at 1100 °C was determined to be between 5.5 GPa (at 20 N) and 8.6 GPa (at 0.5 N), which is in the range of other analyzed SiOC systems.[25,38,39] Furthermore, for the SiOC ceramic produced upon pyrolysis at 1100 °C, nanoindentation investigation revealed a hardness value of 8.6 GPa and a Young's modulus of 66 GPa. Also the Young's modulus of the SiOC ceramic was found to be similar to that of other silicon oxycarbide glasses (50–90 GPa).[23,25,40]

The electrical dc resistivity at room temperature of the SiOC ceramic produced at 1100 °C was 0.35 Ω m as analyzed by the linear four-point probe method, whereas the sample pyrolyzed at 1400 °C showed an even lower dc resistivity of 0.14 Ω m. These values are much lower than those of other SiOC systems (10^7–10^{10} Ω m)[41] and can be explained by the high content of free carbon (turbostratic carbon, graphite-dc resistivity of 1–10^{-5} Ω m)[37] present within the ceramic. This result supports

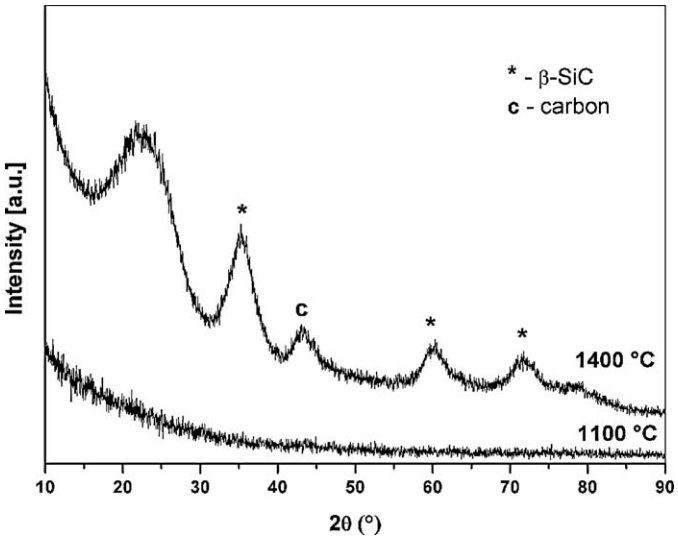

Fig. 7. X-ray powder diffraction patterns of SiOC ceramics pyrolyzed at 1100 and 1400 °C (*—β-SiC; C—carbon).

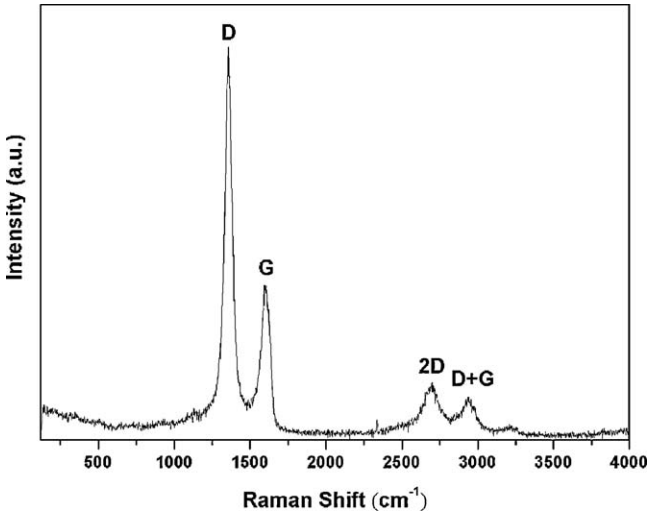

Fig. 8. Raman spectrum of the SiOC ceramic pyrolyzed at 1400 °C.

the TEM investigation, which indicates the presence of a percolation network of turbostratic carbon being responsible for the electrical conductivity of the samples.

4. Conclusions

Crack-free and fully dense silicon oxycarbide ceramic parts were prepared pressureless via direct UV-light crosslinking and subsequent pyrolysis of a commercially available polysiloxane. Whereas pressure-assisted techniques furnish dense ceramics with only simple geometries, the preparation method presented in this paper allows the production of parts with complex shapes; results related to this will be published in a separate paper.[42] Thus, crack-free bulk SiOC ceramic discs with a diameter of 34 mm and a thickness as high as 1.5 mm were produced. The ceramic parts exhibited a rather low density (1.6–1.7 g/cm^3), which was attributed to their high content of carbon, the highest reported yet for silicon oxycarbide ceramics prepared from single-source precursors. The high content of segregated turbostratic carbon present in the SiOC ceramic was also supported by electron microscopy and Raman spectroscopy studies as well as by dc resistivity measurements. Annealing at 1400 °C leads to homogeneous dispersion of nanosized β-SiC crystallites throughout the SiOC matrix, embedded in a percolation network of turbostratic carbon.

Acknowledgements

The authors thank the European Community FP6 (MCRTN-019601, PolyCerNet), and the Federal Ministry of Education and Research (BMBF, Berlin, Germany-project INFUNK) for financial support. The authors also acknowledge Ms. C. Fasel (TGA/MS), Dr. L. Toma (XRD and Raman spectroscopy), Mr. R.M. Prasad (BET), and Mr. K. Flittner (electrical resistivity) for their support throughout the individual measurements. Mrs. K. Böhling is acknowledged for proofreading.

References

1. Colombo P, Mera G, Riedel R, Soraru GD. Polymer-derived ceramics: 40 years of research and innovation in advanced ceramics. *J Am Ceram Soc* 2010;**93**:1805–37.
2. Riedel R, Ionescu E, editors. Special triple issue on"preceramic polymer". *Soft Mater* 2006;**4**(1–3):105–299.
3. Ionescu E, Gervais C, Babonneau F. Polymer-to-ceramic transformation. In: Colombo P, Riedel R, Soraru GD, Kleebe HJ, editors. *Polymer derived ceramics: from nano-structure to applications*. Pennsylvania: Destech Publications; 2010. p. 108–26.
4. Greil P, Seibold M. Modelling of dimensional changes during polymer–ceramic conversion for bulk component fabrication. *J Mater Sci* 1992;**27**:1053–60.
5. Greil P. Active-filler-controlled pyrolysis of preceramic polymers. *J Am Ceram Soc* 1995;**78**:835–48.
6. Riedel R, Toma L, Fasel C, Miehe G. Polymer-derived mullite-SiC-based nanocomposites. *J Eur Ceram Soc* 2009;**29**:3079–90.
7. Greil P. Near net shape manufacturing of polymer derived ceramics. *J Eur Ceram Soc* 1998;**18**:1905–14.
8. Vakifahmetoglu C, Colombo P. A Direct method for the fabrication of macro-porous SiOC ceramics from preceramic polymers. *Adv Eng Mater* 2008;**10**:256–9.
9. Harshe R, Balan C, Riedel R. Amorphous Si(Al)OC ceramic from polysiloxanes: bulk ceramic processing, crystallization behavior and applications. *J Eur Ceram Soc* 2004;**24**:3471–82.
10. Shah SR, Raj R. Mechanical properties of a fully dense polymer derived ceramic made by a novel pressure casting process. *Acta Mater* 2002;**50**:4093–103.
11. Janakiraman N, Aldinger F. Fabrication and characterization of fully dense Si–C–N ceramics from a poly (ureamethylvinyl) silazanes precursor. *J Eur Ceram Soc* 2009;**29**:163–73.
12. Ishihara S, Gu H, Bill J, Aldinger F, Wakai F. Densification of precursor-derived Si–C–N ceramics by high-pressure hot isostatic pressing. *J Am Ceram Soc* 2002;**85**:1706–12.
13. Esfehanian M, Oberacker R, Fett T, Hoffmann MJ. Development of dense filler-free polymer-derived SiOC ceramics by field-assisted sintering. *J Am Ceram Soc* 2008;**91**:3803–5.
14. Riedel R, Passing G, Schönfelder H, Brook RJ. Synthesis of dense silicon based ceramics at low temperatures. *Nature* 1992;**355**:714–6.
15. Seitz J, Bill J. Production of compact polysilazane-derived Si–C–N ceramics by plastic forming. *J Mater Sci Lett* 1996;**15**:391–3.
16. Konetschny C, Galusek D, Reschke S, Fasel C, Riedel R. Dense silicon carbonitride ceramics by pyrolysis of crosslinked and warmpressed polysilazane powders. *J Eur Ceram Soc* 1999;**19**:2789–96.

17. Ionescu E, Linck C, Fasel C, Müller M, Kleebe HJ, Riedel R. Polymer-derived SiOC/ZrO_2 ceramic nanocomposites with excellent high-temperature stability. *J Am Ceram Soc* 2010;**93**:241–50.
18. Ionescu E, Papendorf B, Kleebe HJ, Riedel R. Polymer-derived silicon oxycarbide/hafnia ceramic nanocomposites. Part II: stability toward decomposition and microstructure evolution at T » 1000 °C. *J Am Ceram Soc* 2010;**93**:1783–9.
19. Ionescu E, Stoyanov E, Navrotsky A, Riedel R, unpublished results.
20. Ionescu E, Papendorf B, Kleebe HJ, Poli F, Müller J, Riedel R. Polymer derived silicon oxycarbide/hafnia ceramic nanocomposites Part I: phase and microstructure evolution during the ceramization process. *J Am Ceram Soc* 2010;**93**:1774–82.
21. Kleebe HJ, Blum YD. SiOC ceramic with excess free carbon. *J Eur Ceram Soc* 2008;**28**:1037–42.
22. Rouxel T, Massouras G, Soraru GD. High-temperature behavior of a SiOC oxycarbide glass: elasticity and viscosity. *J Sol–Gel Sci Technol* 1999;**14**:83–94.
23. Mera M, Riedel R, Poli F, Müller K. Carbon-rich SiCN Ceramics derived from phenyl containing poly (silylcarbodiimides). *J Eur Ceram Soc* 2009;**29**:2873–83.
24. Blum YD, MacQueen DB, Kleebe HJ. Synthesis and characterization of carbon-enriched silicon oxycarbides. *J Eur Ceram Soc* 2005;**25**:143–9.
25. Segatelli MG, Pires ATM, Yoshida IVP. Synthesis and structural characterization of carbon-rich SiC_xO_y derived from a Ni-containing hybrid polymer. *J Eur Ceram Soc* 2008;**28**:2247–57.
26. Renlund GM, Prochazka S, Doremus RH. Silicon oxycarbide glasses. Part II: structure and properties. *J Mater Res* 1991;**6**:2716–22.
27. Su D, Li YL, An HJ, Liu X, Hou F, Li JY, et al. Pyrolytic transformation of liquid precursors to shaped bulk ceramics. *J Eur Ceram Soc* 2010;**30**:1503–11.
28. Moysan C, Riedel R, Harshe R, Rouxel T, Augereau T. Mechanical characterization of a polysiloxane-derived SiOC glass. *J Eur Ceram Soc* 2007;**27**:397–403.
29. Galusek D, Riley FL, Riedel R. Nanoindentation of a polymer-derived amorphous silicon carbonitride ceramic. *J Am Ceram Soc* 2001;**84**:1164–6.
30. Rino JP, Ebbsjö I, Branicio PS, Kalia RK, Nakano A, Shimojo F, et al. Short- and intermediate-range structural correlations in amorphous silicon carbide: a molecular dynamics study. *Phys Rev B* 2004;**70**:045207.
31. www.pyrocarbon.de.
32. Gregori G, Kleebe HJ, Blum YD, Babonneau F. Evolution of C-rich SiOC ceramics. Part II: characterization by high lateral resolution techniques: electron energy-loss spectroscopy, high-resolution TEM and energy filtered TEM. *Int J Mater Res* 2006;**97**:710–20.
33. Strömer H, Kleebe HJ, Ziegler G. Metastable SiCN glass matrices studied by energy-filtered electron diffraction pattern analysis. *J Non Cryst Solids* 2007;**353**:2181–7.
34. Li ZQ, Lu CJ, Xia ZP, Zhou Y, Luo Z. X-Ray diffraction patterns of graphite and turbostratic carbon. *Carbon* 2007;**45**:1686–95.
35. Ferrari AC, Robertson J. Interpretation of Raman spectra of disordered and amorphous carbon. *Phys Rev B* 2000;**61**:14095–107.
36. Pimenta AM, Dresselhaus G, Dresselhaus MS, Cançado LG, Jorio A, Saito R. Studying disorder in graphite-based systems by Raman spectroscopy. *Phys Chem Chem Phys* 2007;**9**:1276–90.
37. Ferrari AC. Raman spectroscopy of graphene and graphite: disorder, electron-phonon coupling doping and nonadiabatic effects. *Sol State Commun* 2007;**143**:47–57.
38. Soraru GD, Dallapiccola E, D'Andrea G. Mechanical characterization of sol–gel derived silicon oxycarbide glasses. *J Am Ceram Soc* 1996;**79**:2074–80.
39. Walter S, Soraru GD, Brequel H, Enzo S. Microstructural and mechanical characterization of sol–gel derived SiOC glasses. *J Eur Ceram Soc* 2002;**22**:2389–400.
40. Chen LF, Cai ZH, Zhang L, Lan, Chen XJ, Zheng J. Preparation and properties of silicon oxycarbide fibers. *J Mater Sci* 2007;**42**:1004–9.
41. Cordelair J, Greil P. Electrical conductivity measurements as a microprobe for structure transitions in polysiloxane derived Si–O–C ceramics. *J Eur Ceram Soc* 2000;**20**:1947–57.
42. Ionescu E, Martínez Crespiera S, Riedel R, unpublished results.